Journal of ELECTRICAL ENGINEERING, VOL 70 (2019), NO-7S, 71–76

sciendo

PAPERS

Magnetic properties of hematite ($\alpha - Fe_2O_3$) nanoparticles synthesized by sol-gel synthesis method: The influence of particle size and particle size distribution

Marin Tadic[*], Matjaz Panjan[**], Biljana Vucetic Tadic[***], Jelena Lazovic[****], Vesna Damnjanovic[⊞], Martin Kopani[⊞⊞], Lazar Kopanja[⊞⊞⊞,⊞⊞⊞⊞]

Using the sol-gel method we synthesized hematite ($\alpha - Fe_2O_3$) nanoparticles in a silica matrix with 60 wt % of hematite. X-ray diffraction (XRD) patterns and Fourier transform infrared (FTIR) spectra of the sample demonstrate the formation of the $\alpha - Fe_2O_3$ phase and amorphous silica. A transmission electron microscopy (TEM) measurements show that the sample consists of two particle size distributions of the hematite nanoparticles with average sizes around 10 nm and 20 nm, respectively. Magnetic properties of hematite nanoparticles were measured using a superconducting quantum interference device (SQUID). Investigation of the magnetic properties of hematite nanoparticles showed a divergence between field-cooled (FC) and zero-field-cooled (ZFC) magnetization curves and two maxima. The ZFC magnetization curves displayed a maximum at around $T_B = 50$ K (blocking temperature) and at $T_M = 83$ K (the Morin transition). The hysteresis loop measured at 5 K was symmetric around the origin, with the values of coercivity, remanent and mass saturation magnetization $H_{C10K} \approx 646$ A/cm, (810 Oe), $M_{r10K} = 1.34$ emu/g and $M_{S10K} = 6.1$ emu/g respectively. The absence of both coercivity ($H_{C300K} = 0$) and remanent magnetization ($M_{r300K} = 0$) in $M(H)$ curve at 300 K reveals super-paramagnetic behavior, which is desirable for application in biomedicine. The bimodal particle size distributions were used to describe observed magnetic properties of hematite nanoparticles. The size distribution directly influences the magnetic properties of the sample.

K e y w o r d s: iron oxide, hematite ($\alpha - Fe_2O_3$), sol-gel synthesis, superparamagnetism (SPION), Morin transition, particle size effects

1 Introduction

The investigations of iron(III) oxide nanoparticles and their physical properties have attracted considerable attention in recent years [1-10]. Iron(III) oxides show remarkable magnetic properties, both for fundamental investigations and practical applications. The magnetic properties of these materials have been shown to depend on their size, shape, and microstructure [11-16]. In particular, iron(III) oxides are an attractive group of materials with a wide range of magnetic properties, from antiferromagnetic, superparamagnetic and weak ferromagnetic to ferrimagnetic [17-30]. As the size of the particles decreases, the magnetic properties of the iron(III) oxides exhibit peculiar properties, which differ from those of bulk counterpart materials, because of nanoscale confinement and surface effects. They have a range of practical applications in different technological areas, such as solar cell, pigment, microwave absorption, catalysis, environment protection, gas sensor, magnetic storage, clinical diagnosis and treatment, etc [31-40].

Among the iron(III) oxides hematite is the most thermally stable polymorph. Hematite crystallizes in the rhombohedral system, space group R-3c [40]. Bulk hematite is a weak ferromagnet below the Néel temperature T_N ($948 < T_N < 963$ K) that undergoes a magnetic phase transition at the Morin temperature T_M ($T_M \approx 263$ K) to a purely antiferromagnetic phase at lower temperatures [40]. Hematite magnetic properties depend on the particle size and display the most interesting effects when the size of the particles decreases below 20 nm. The Morin temperature reduces with decreases of the particle size and tends to vanish for particles smaller than about 10 nm [41,42]. A reduction of the Néel temperature with decreasing particle size has been also observed [43]. If the particles become small enough, the direction of the magnetic moment in a single domain fluctuates due to thermal agitation, leading to superparamagnetic be-

*Condensed Matter Physics Laboratory, Vinca Institute, University of Belgrade, POB 522, 11001 Belgrade, Serbia, marint@vinca.rs, **Jožef Stefan Institute, Jamova 39, 1000 Ljubljana, Slovenia, ***Institute for Mother and Child Healthcare of Serbia, Belgrade, Serbia, ****Vienna Biocenter Core Facilities, Vienna, Austria, ⊞Department of Physics, University of Belgrade, Faculty of Mining and Geology, Belgrade, Serbia, ⊞⊞Institute of Medical Physics, Biophysics, Informatics and Telemedicine, Faculty of Medicine, Comenius University, Bratislava, Slovakia, ⊞⊞⊞Faculty of Technology and Metallurgy, University of Belgrade, Belgrade, Serbia, ⊞⊞⊞⊞Faculty of Mathematics and Computer Science, Alfa BK University, Palmira Toljatija 3, 11070 Belgrade, Serbia,

DOI: 10.2478/jee-2019–0044, Print (till 2015) ISSN 1335-3632, On-line ISSN 1339-309X

haviour above the blocking temperature T_B, and to spatial freezing of these moments below T_B [44,45]. Several recent studies have been focused on understanding the influence of the particle sizes on the magnetic properties of hematite. These studies have shown that the particle size of $\alpha - Fe_2O_3$ nanoparticles has a significant impact on the magnetic properties, in particular on the Morin transition, the Néel temperature and superparamagnetic relaxation of the nanoparticles [43,46]. Consequently, synthesis methods and systems where the size of magnetic nanoparticles can be changed in a controllable manner are the most useful for studying the above-described effects.

In our previous papers [44,45], we reported on a study of $\alpha - Fe_2O_3/SiO_2$ nanocomposites containing 30 wt% and 45 wt% of hematite prepared by the sol-gel method. The results revealed the existence of single particle size distribution and no evidence of significant particle agglomeration. In this work, we present continuation of our investigations of highly concentrated hematite nanoparticles (60% in weight) in a silica matrix obtained by the same preparation method. The results on the structural and magnetic properties collected by using X-ray powder diffraction (XRPD), transmission electron microscopy (TEM) and magnetization measurements are presented. The observed magnetic properties classify the investigated sample in the superparamagnetic (the blocking temperature) and weak ferromagnetic (the Morin transition). The particle size distribution has been taken into account in the study on the nanoscale size-effects of magnetic properties.

2 Experiment

The Fe_2O_3/SiO_2 nanocomposite was prepared by the sol-gel method [44,45]. The starting point for the synthesis of was a solution prepared by mixing tetraethyl orthosilicate (TEOS), deionized water and ethanol. An aqueous solution of iron nitrate ($Fe(NO_3)_3$ $9H_2O$ vv, Aldrich 98%) was added to the initial solution in such a proportion as to provide 60 wt% of iron oxide in the final dried powder. The subsequent heat treatment of the sample was carried out in the air for 5 h at 200 °C.

The crystal structure was analyzed by X-ray powder diffraction (XRPD) on a Rigaku RINT-TTRIII diffractometer operating with Cu K_α radiation. Measurements were performed in range $2\theta = 10 - 80\,°$. The particle size and size distribution were investigated using TEM (transmission electron microscopy, JEOL 2010F). Fourier Transform Infrared (FTIR) spectra of samples were recorded on a Nicolet FTIR spectrometer (IS 50) at room temperature in the wavenumber range of $4000 - -400$ cm^{-1} with a resolution of 4 cm^{-1}. Magnetic measurements were performed on a commercial Quantum Design MPMS-XL-5 superconducting quantum interference device (SQUID)-based magnetometer in a wide range of temperatures ($5 - 300$ K) and applied DC fields (up to 5 T).

3 Results and discussion

The crystal structure and the phase composition of the sample were examined by X-ray diffraction (XRD) measurements. The recorded diffraction pattern and indexed peaks are shown in Fig. 1.

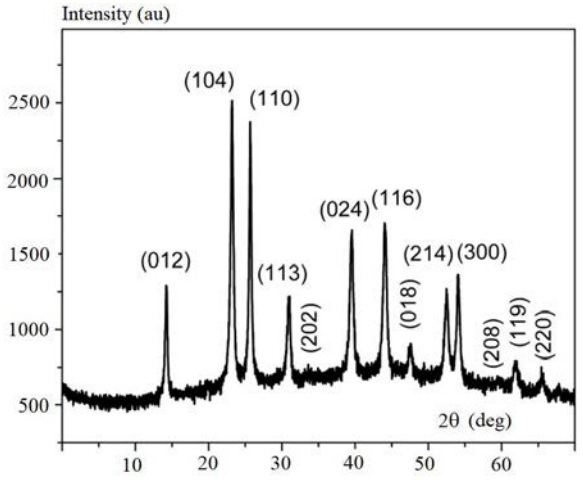

Fig. 1. X-ray diffraction pattern of the sample and the Miller indices (hkl) of the peaks

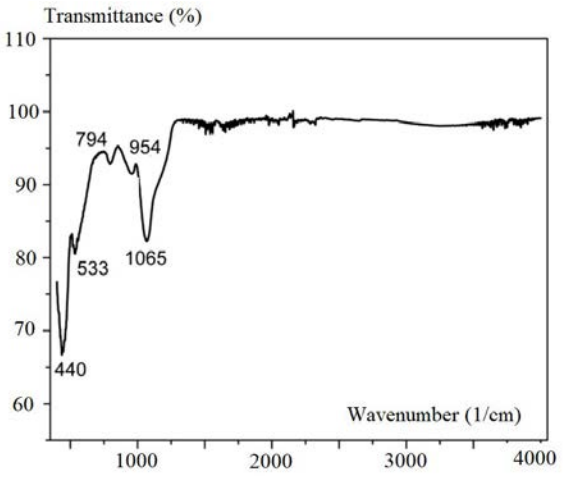

Fig. 2. FTIR spectrum of hematite/SiO_2 nanostructure

The broad diffraction peaks can be observed, as expected for nanocrystalline particles. The positions of all the peaks coincide with the maxima characteristic of the hematite phase (JCPDS card 33-0664). No diffraction line corresponding to other phases has been observed, indicating high purity of the sample. The FTIR spectrum of the sample was shown in Fig. 2. Two absorption peaks at about 533 and 440 cm^{-1} are observed in the spectrum of the sample. In comparison with the literature, we conclude that these peaks corresponded to the stretching and bending modes of the Fe-O bond in hematite [47]. The peaks located at 1065 and 794 cm^{-1} are assigned, respectively, to the asymmetric and symmetric stretching of SiOSi [48,49]. The absorption band at 954 cm^{-1} can

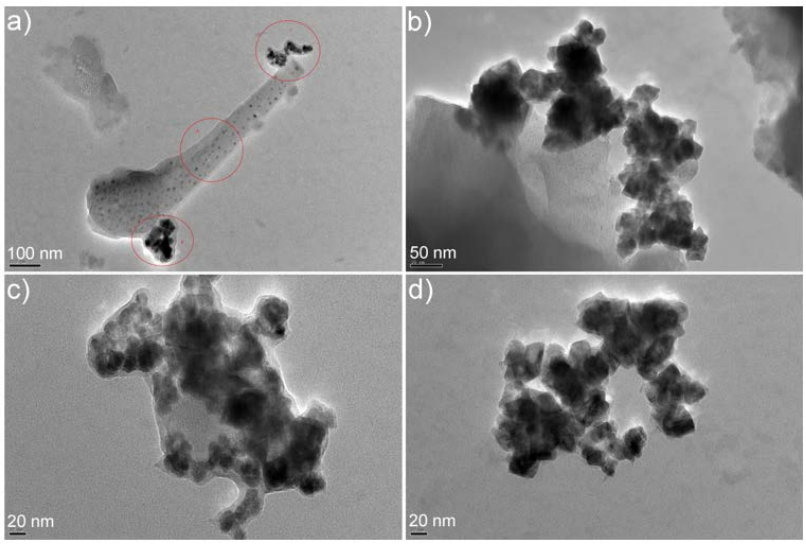

Fig. 3. TEM images of hematite/SiO_2 nanostructure

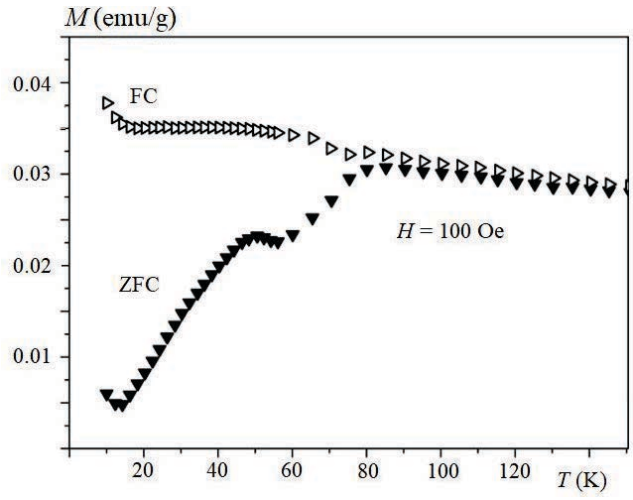

Fig. 4. Temperature dependence of the zero-field-cooled (ZFC, solid symbols) and field-cooled (FC, open symbols) magnetization measured in a field of 80 A/cm (100 Oe)

be assigned to SiOH stretching vibration [50]. No peaks that would correspond to other iron oxide phases were observed, indicating a pure hematite phase has formed. The particle size and particle size distribution of the as-prepared $\alpha - Fe_2O_3$ powder were studied by transmission electron microscopy. The TEM micrographs for the sample are shown in Fig. 3. It can be seen that the powder is composed of particles with average sizes of about 10 and 20 nm, respectively. Therefore, this nanoparticle system has a broad particle size distribution that consists of two distinct particle size distributions (bi-modal system).

Magnetic nanoparticles with sizes below 100 nm in diameter represent an interesting group of materials where their magnetic properties depend on their size. The relaxation of the magnetization orientation of each particle is determined by $\tau = \tau_0 e^{KV/2kT}$, in which τ is the relaxation time at one orientation, τ_0 is attempt frequency, K is the particles anisotropy constant, V is the particle volume, k is Boltzmanns constant, and T is temperature [51]. The energy barrier between the two orientations is $\sim KV$. Decreasing the size of the particle up to $KV \leq KT$ (KT-thermal energy) the particles magnetization starts to fluctuate from one direction to another and this state is called superparamagnetic (the magnetic moment of this particle is randomized to zero). The magnetic state of the magnetic nanoparticles can be investigated by measuring M (magnetization) *vs* H (applied magnetic field). For the superparamagnetic state under an applied magnetic field $H = 0$, the magnetization of each magnetic particle points in different directions and the overall magnetic moment is zero [51]. The typical properties of a superparamagnetic material are the existence of a blocking temperature T_B, irreversibility (*ie* , bifurcation) of the ZFC and FC curves at T_{irr} (irreversibility temperature) and the absence of the magnetic hysteresis above T_B (superparamagnetism). On the other hand, for the ferromagnetic particles typical properties are the remanent magnetization ($M_r > 0$) and coercivity ($H_C > 0$). The $M(T)$ of hematite may display three interesting temperatures for investigation: the Néel temperature, the Morin temperature, and the blocking temperature [41-43, 52-55]. The measured $M(T)$ dependence for the sample is shown in Fig. 4, where ZFC magnetization sharply increases at 54 K, reaching a maximum at 83 K with a subsequent decrease up to 300 K.

This sharp jump and behavior of the magnetization is the property of $\alpha - Fe_2O_3$ phase and is called the Morin transition [52,53]. Moreover, a blocking temperature at about 50 K that originates from the $\alpha - Fe_2O_3$ nanoparticles is also visible in the ZFC curve, thus indicating the presence of the nanoparticles with smaller sizes. These magnetic properties of the sample can be explained by the bimodal particle size distributions that are observed in TEM images (Fig. 3). The group of the

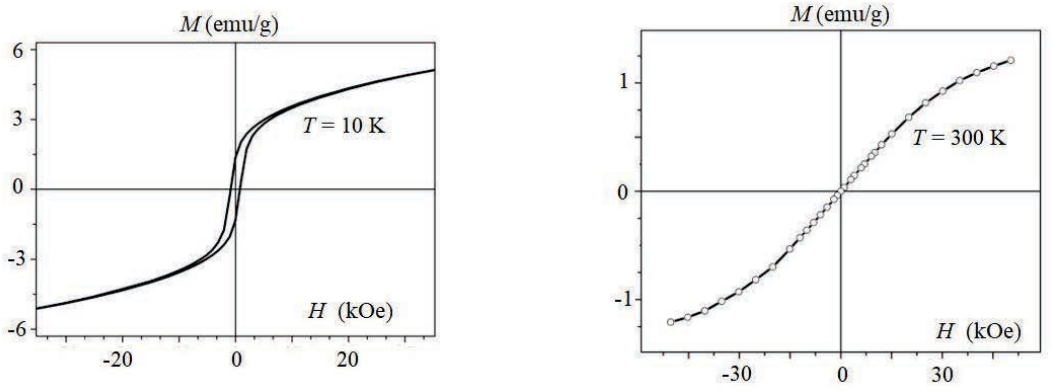

Fig. 5. Magnetization *vs* applied magnetic field recorded at: (a) – 10, and (b) – at 300 K, (1 kOe = 800 A/cm)

particles with sizes around 10 nm produced blocking temperature whereas the particles with higher sizes around 20 nm produced the Morin transition (Fig. 3). Fig. 5(a) shows the field dependence of the isothermal magnetization $M(H)$ at 10 K. Absence of the magnetization saturation as well as the existence of the hysteresis loop below the blocking temperature should be noticed. The values of the coercivity, remanent, and mass saturation magnetization are $H_{C10K} = 646$ A/cm (810 Oe), $M_{r10K} = 1.34$ emu/g and $M_{S10K} = 6.1$ emu/g, respectively. (NOTE: emu/g $= Am^2/kg$). The $M(H)$ measurements were also recorded at $T = 300$ K for the sample (Fig. 5(b)). The absence of both coercivity ($H_{C300K} = 0$) and remanent magnetization ($M_{r300K} = 0$) suggests superparamagnetic behavior at this temperature. The value of the saturation magnetization of the sample was $M_{S300K} = 1.93$ emu/g at 300 K. The values of M_S were determined by extrapolating $1/H$ to zero-field in the M *vs* $1/H$ plot based on the high field data. The bimodal particle size distributions observed by TEM measurements (Fig. 3) were used to describe the magnetic properties of hematite nanoparticles. This suggests that particles with smaller sizes around 10 nm produced blocking temperature and superparamagnetism, whereas particles around 20 nm produced the Morin transition.

4 Conclusion

The $\alpha - Fe_2O_3/SiO_2$ nanostructure containing 60 wt% of hematite were synthesized by the sol-gel method and characterized by XRD, FTIR, TEM, and SQUID magnetometer. The XRD and FTIR revealed the formation of the hematite phase and amorphous silica. The TEM measurements show hematite nanoparticles with a wide range of particle sizes embedded in silica matrix and bimodal particle size distributions. The iron oxide nanocrystals with bimodal size distributions and average diameters around 10 and 20 nm allowed us to directly investigate the size-dependent magnetic properties of hematite. We observed both the Morin transition and blocking temperature (both of them are size-dependent magnetic properties), which can be attributed to the bimodal size distributions. The Morin transition is a result of the particles with sizes around 20 nm whereas the blocking temperature is a consequence of the particles around 10 nm. The magnetic behavior of the sample clearly demonstrated the effects of the particle size, especially on the magnetization dependence on the temperature $M(T)$. We conclude that the dimensionality and the size distribution of the nanoparticles are two main factors that determine the magnetic properties of the synthesized sample.

Acknowledgements

The Ministry of Education, Science and Technology of the Republic of Serbia supported this work financially (Grants nos. III 45015 and III 044006). The support by the Ministry of Higher Education, Science and Technology of the Republic of Slovenia within the National Research Program is acknowledged. We would also like to acknowledge Serbian-Slovenian bilateral project BI-RS/16-17-030, Serbian-Austrian bilateral project 451-03-02141/2017-09/10, bilateral project BI-RS/16-17-030 and Serbia-Slovakia bilateral project SK-SRB-2016-0055.

References

[1] G. Kandasamy, A. Sudame, P. Bhati, A. Chakrabarty, S. N. Kale, and D. Maity, "Systematic magnetic fluid hyperthermia studies of carboxyl functionalized hydrophilic superparamagnetic iron oxide nanoparticles based ferrofluids", *Journal of colloid and interface science*, vol. 514, pp. 534–543, 2018.

[2] G. Kandasamy, A. Sudame, T. Luthra, K. Saini and D. Maity, "Functionalized hydrophilic superparamagnetic iron oxide nanoparticles for magnetic fluid hyperthermia application in liver cancer treatment", *ACS Omega*, vol. 3, pp. 3991–4005, 2018.

[3] S. M. Suturin, A. M. Korovin, S. V. Gastev, M. P. Volkov, A. A. Sitnikova, D. A. Kirilenko, M. Tabuchi and N. S. Sokolov, "Tunable polymorphism of epitaxial iron oxides in the four-in-one ferroic-on-GaN system with magnetically ordered α-, γ-, ε-Fe2O3, and Fe3O4 layers", *Physical Review Materials*, vol. 2, pp. 073 -403, 2018.

[4] M. Tadic, I. Milosevic, S. Kralj, M. Mitric, D. Makovec, M. L. Saboungi and L. Motte, "Synthesis of metastable hard-magnetic ε-Fe2O3 nanoparticles from silica-coated akaganeite nanorods", *Nanoscale*, vol. 9, pp. 10579–10584, 2017.

[5] M. Tadic, S. Kralj and L. Kopanja, "Synthesis, particle shape characterization and surface modification of superparamagnetic iron oxide nanochains", *Materials Characterization*, vol. 148, pp. 123–133, 2019.

[6] M. Tadic, S. Kralj, Y. Lalatonne and L. Motte, "Iron oxide nanochains coated with silica: Synthesis, surface effects and magnetic properties", *Applied Surface Science*, vol. 476, pp. 641–646, 2019.

[7] J. Matmin, I. Affendi, S. Ibrahim and S. Endud, "Additive-free rice starch-assisted synthesis of spherical nanostructured hematite for degradation of dye contaminant", *Nanomaterials*, vol. 8, pp. 702, 2018.

[8] A. Rufus, N. Sreeju, and D. Philip, "Size tunable biosynthesis and luminescence quenching of nanostructured hematite (α-Fe2O3) for catalytic degradation of organic pollutants", *Journal of Physics and Chemistry of Solids*, vol. 124, pp. 221 –234, 2019.

[9] A. S. Hassanien and A. A. Akl, "Optical characteristics of iron oxide thin films prepared by spray pyrolysis technique at different substrate temperatures", *Applied Physics A*, vol. 124, pp. 752, 2018.

[10] Z. Shaoqiang, T. Dong, Z. Geng, H. Lin, Z. Hua, H. Jun, L. Yi, L. Minxia, H. Yaohua and Z. Wei, "The influence of grain size on the magnetic properties of Fe3O4 nanocrystals synthesized by solvothermal method", *Journal of Sol-Gel Science and Technology*, pp. 1–8, 2019.

[11] J. Mohapatra, F. Zeng, K. Elkins, M. Xing, M. Ghimire, S. Yoon, S. R. Mishra and J. P. Liu, "Size-dependent magnetic and inductive heating properties of Fe3O4 nanoparticles: scaling laws across the superparamagnetic size", *Physical Chemistry Chemical Physics*, vol. 20, pp. 12879–12887, 2018.

[12] Z. Nemati, J. Alonso, I. Rodrigo, R. Das, E. Garaio, J. A. García, I. Orue, M. H. Phan and H. Srikanth, "Improving the heating efficiency of iron oxide nanoparticles by tuning their shape and size", *The Journal of Physical Chemistry C*, vol. 122, pp. 2367–2381, 2018.

[13] B. Park, B. H. Kim and T. Yu, "Synthesis of spherical and cubic magnetic iron oxide nanocrystals at low temperature in air", *Journal of colloid and interface science*, vol. 518, pp. 27–33, 2018.

[14] M. Bhushan, Y. Kumar, L. Periyasamy and A. K. Viswanath, "Facile synthesis of Fe/Zn oxide nanocomposites and study of their structural, magnetic, thermal, antibacterial and cytotoxic properties", *Materials Chemistry and Physics*, vol. 209, pp. 233–248, 2018.

[15] A. A. Ati, "Fast synthesis, structural, morphology with enhanced magnetic properties of cobalt doped nickel ferrite nanoscale", *Journal of Materials Science: Materials in Electronics*, vol. 29, pp. 12010–12021, 2018.

[16] E. Aubry, T. Liu, A. Dekens, F. Perry, S. Mangin, T. Hauet and A. Billard, "Synthesis of iron oxide films by reactive magnetron sputtering assisted by plasma emission monitoring", *Materials Chemistry and Physics*, vol. 223, pp. 360–365, 2019.

[17] R. E. Elshater, G. Kawamura, F. Fakhry, T. Meaz, M. A. Amer and A. Matsuda, "Structural phase transition of spinel to hematite of as-prepared Fe2+-Cr nanoferrites by sintering temperature", *Measurement*, vol. 132, pp. 272–281, 2019.

[18] D. Kubániová, L. Kubíčková, T. Kmječ, K. Závěta, D Nižňanský, P. Brázda, M. Klementová and J. Kohout, "Hematite: Morin temperature of nanoparticles with different size", *Journal of Magnetism and Magnetic Materials*, vol. 475, pp. 611–619, 2019.

[19] M. Tadic, S. Kralj, M. Jagodic, D. Hanzel and D. Makovec, "Magnetic properties of novel superparamagnetic iron oxide nanoclusters and their peculiarity under annealing treatment", *Applied Surface Science*, vol. 322, pp. 255–264, 2014.

[20] A. Lassoued, M. S. Lassoued, B. Dkhil, S. Ammar and A. Gadri, "Synthesis, photoluminescence and Magnetic properties of iron oxide (α-Fe2O3) nanoparticles through precipitation or hydrothermal methods", *Physica E: Low-dimensional Systems and Nanostructures*, vol. 101, pp. 212–219, 2018.

[21] O. S. Ivanova, R. D. Ivantsov, I. S. Edelman, E. A. Petrakovskaja, D. A. Velikanov, Y. V. Zubavichus, V. I. Zaikovskii and S. A. Stepanov, "Identification of ε-Fe2O3 nano-phase in borate glasses doped with Fe and Gd", *Journal of Magnetism and Magnetic Materials*, vol. 401, pp. 880–889, 2016.

[22] A. Nikitin, M. Khramtsov, A. Garanina, P. Mogilnikov, N. Sviridenkova, I. Shchetinin, A. Savchenko, M. Abakumov and A. Majouga, "Synthesis of iron oxide nanorods for enhanced magnetic hyperthermia", *Journal of Magnetism and Magnetic Materials*, vol. 469, pp. 443–449, 2019.

[23] M. P. Zaytseva, A. G. Muradova, A. I. Sharapaev, E. V. Yurtov, I. S. Grebennikov and A. G. Savchenko, "Fe3O4/SiO2 Core Shell Nanostructures: Preparation and Characterization", *Russian Journal of Inorganic Chemistry*, vol. 63, pp. 1684–1688, 2018.

[24] D. Z. Tulebayeva, A. L. Kozlovskiy, I. V. Korolkov, Y. G. Gorin, A. V. Kazantsev, L. Abylgazina, E. E. Shumskaya, E. Y. Kaniukov and M. V. Zdorovets, "Modification of Fe3O4 nanoparticles with carboranes", *Materials Research Express*, vol. 5, pp. 105011, 2018.

[25] M. V. Efremova, Y. A. Nalench, E. Myrovali, A. S. Garanina, I. S. Grebennikov, P. K. Gifer, M. A. Abakumov, M. Spasova, M. Angelakeris, A. G. Savchenko and M. Farle, "Size-selected Fe_3O_4Au hybrid nanoparticles for improved magnetism-based theranostics", *Beilstein journal of nanotechnology*, vol. 9, pp. 2684–2699, 2018.

[26] P. Veverka, M. Pashchenko, L. Kubíčková , J. Kuličková, Z. Jirák, R. Havelek, K. Královec, J. Kohout and O. Kaman, "Rod-like particles of silica-coated maghemite: synthesis via akaganeite, characterization and biological properties", *Journal of Magnetism and Magnetic Materials*, vol. 476, pp. 149–156, 2019.

[27] I. Shanenkov, A. Sivkov, A. Ivashutenko, T. Medvedeva and I. Shchetinin, "High-energy plasma dynamic synthesis of multiphase iron oxides containing Fe3O4 and ε-Fe2O3 with possibility of controlling their phase composition", *Journal of Alloys and Compounds*, vol. 774, pp. 637–645, 2019.

[28] S. S. Yakushkin, D. A. Balaev, A. A. Dubrovskiy, S. V. Semenov, Y. V. Knyazev, O. A. Bayukov, V. L. Kirillov, R. D. Ivantsov, I. S. Edelman and O. N. Martyanov, "ε-Fe2O3 nanoparticles embedded in silica xerogelMagnetic metamaterial", *Ceramics International*, vol. 44, pp. 17852–17857, 2018.

[29] M. Krajewski, K. Brzozka, M. Tokarczyk, G. Kowalski, S. Lewinska, A. Slawska-Waniewska, W. S. Lin and H. M. Lin, "Impact of thermal oxidation on chemical composition and magnetic properties of iron nanoparticles", *Journal of Magnetism and Magnetic Materials*, vol. 458, pp. 349–354, 2018.

[30] H. Mansour, R. Bargougui, C. Autret-Lambert, A. Gadri and S. Ammar, "Co-precipitation synthesis and characterization of tin-doped α-Fe2O3 nanoparticles with enhanced photocatalytic activities", *Journal of Physics and Chemistry of Solids*, vol. 114, pp. 1–7, 2018.

[31] F. Bouhjar, M. Mollar, S. Ullah, B. Marí and B. Bessais, "Influence of a Compact α-Fe2O3 Layer on the Photovoltaic Performance of Perovskite-Based Solar Cells", *Journal of The Electrochemical Society*, vol. 165(2), pp. H30–H38, 2018.

[32] C. Busabok, W. Khongwong, P. Somwongsa, P. Ngernchuklin, A. Saensing and S. Kanchanasutha, "Preparation of Near-Infrared (NIR) Reflective Pigment by Solid State Reaction between Fe2O3 and Al2O3", *Key Engineering Materials*, vol. 766, pp. 127–132, 2018.

[33] J. Ji, Y. Huang, J Yin, X. Zhao, X. Cheng, S. He, X. Li, J. He and J. Liu, "Synthesis and Electromagnetic and Microwave Absorption Properties of Monodispersive Fe3O4/α-Fe2O3 Composites", *ACS Applied Nano Materials*, vol. 1, pp. 3935–3944, 2018.

[34] L. Chen, X. Zuo, S. Yang, T. Cai and D. Ding, "Rational design and synthesis of hollow Co3O4@Fe2O3 core-shell nanostructure for the catalytic degradation of norfloxacin by coupling with

peroxymonosulfate", *Chemical Engineering Journal*, vol. 359, pp. 373–384, 2019.

[35] H. Xu, X. Zhang and Y. Zhang, "Modification of biochar by Fe2O3 for the removal of pyridine and quinoline", *Environmental technology*, vol. 39, pp. 1470–1480, 2018.

[36] E. Dai, P. Wang, Y. Ye, Y. Cai, J. Liu and C. Liang, "Ultrafine nanoparticles conglomerated α-Fe2O3 nanospheres with excellent gas-sensing performance to ethanol molecules", *Materials Letters*, vol. 211, pp. 239–242, 2018.

[37] H. Tokoro, W. Tarora, A. Namai, M. Yoshikiyo and S. I. Ohkoshi, "Direct Observation of Chemical Conversion from Fe3O4 to ε-Fe2O3 by a Nanosize Wet Process", *Chemistry of Materials*, vol. 30, pp. 2888–2894, 2018.

[38] C. Dubreil, O. Sainte Catherine, Y. Lalatonne, C. Journé, P. Ou, P. van Endert. and L. Motte, "Tolerogenic iron oxide nanoparticles in type 1 diabetes: biodistribution and pharmacokinetics studies in nonobese diabetic mice", *Small*, vol. 14, pp. 1802053, 2018.

[39] J. Gupta, A. Prakash, M. K. Jaiswal, A. Agarrwal and D. Bahadur, "Superparamagnetic iron oxide-reduced graphene oxide nanohybrid-a vehicle for targeted drug delivery and hyperthermia treatment of cancer", *Journal of Magnetism and Magnetic Materials*, vol. 448, pp. 332–338, 2018.

[40] A. S. Teja and P. Y. Koh, "Synthesis, properties, and applications of magnetic iron oxide nanoparticles. Progress in crystal growth and characterization of materials", vol. 55, pp.22 –45, 2009.

[41] M. Tadic, D. Markovic, V. Spasojevic, V. Kusigerski, M. Remškar, J. Pirnat and Z. Jagličic, "Synthesis and magnetic properties of concentrated α-Fe2O3 nanoparticles in a silica matrix", *Journal of alloys and compounds*, vol. 441, pp. 291–296, 2007.

[42] M. Tadic, V. Kusigerski, D. Markovic, I. Milosevic and V. Spasojevic, "High concentration of hematite nanoparticles in a silica matrix: structural and magnetic properties", *Journal of Magnetism and Magnetic Materials*, vol. 321, pp. 12–16, 2009.

[43] H. M. Lu and X. K. Meng, "Morin temperature and Néel temperature of hematite nanocrystals", *The Journal of Physical Chemistry C*, vol. 114, pp. 21291–21295, 2010.

[44] M. Tadic, M. Panjan, V. Damnjanovic and I. Milosevic, "Magnetic properties of hematite (α-Fe2O3) nanoparticles prepared by hydrothermal synthesis method", *Applied Surface Science*, vol. 320, pp. 183–187, 2014.

[45] L. Kopanja, I. Milosevic, M. Panjan, V. Damnjanovic and M. Tadic, "Solgel combustion synthesis, particle shape analysis and magnetic properties of hematite (α-Fe2O3) nanoparticles embedded in an amorphous silica matrix", *Applied Surface Science*, vol. 362, pp. 380–386, 2016.

[46] J. Fock, M. F. Hansen, C. Frandsen and S. Morup, "On the interpretation of M$^{\boxplus\boxplus}$ossbauer spectra of magnetic nanoparticles", *Journal of Magnetism and Magnetic Materials*, vol. 445, pp. 11–21, 2018.

[47] D. Trpkov, M. Panjan, L. Kopanja and M. Tadic, "Hydrothermal synthesis, morphology, magnetic properties and self-assembly of hierarchical α-Fe2O3 (hematite) mushroom-, cube-and sphere-like superstructures", *Applied Surface Science*, vol. 457, pp. 427 –438, 2018.

[48] K. C. Souza, D. S. M. Nelcy and M. B. S. Edésia, "Mesoporous silica-magnetite nanocomposite: facile synthesis route for application in hyperthermia", *Journal of sol-gel science and technology*, vol. 53, pp. 418–427, 2010.

[49] S. Kralj, M. Drofenik and D. Makovec, "Controlled surface functionalization of silica-coated magnetic nanoparticles with terminal amino and carboxyl groups", *Journal of Nanoparticle Research*, vol. 13, pp. 2829–2841, 2011.

[50] P. Innocenzi, "Infrared spectroscopy of solgel derived silica-based films: a spectra-microstructure overview", *Journal of Non-Crystalline Solids*, vol. 316, pp. 309–319, 2003.

[51] S. Sun, "Recent advances in chemical synthesis, self-assembly, and applications of FePt nanoparticles", *Advanced Materials*, vol. 18, pp. 393–403, 2006.

[52] M. Satheesh, A. R. Paloly, C. K. Krishna Sagar, K. G. Suresh and M. J. Bushiri, "Improved Coercivity of Solvothermally Grown Hematite (α-Fe2O3) and Hematite/Graphene Oxide Nanocomposites (α-Fe2O3/GO) at Low Temperature", *Physica status solidi A*, vol. 215, pp. 1700705, 2018.

[53] M. M. S. Sanad and M. M. Rashad, "Magnetic properties of hematite-titania nanocomposites from ilmenite leachant solutions", *Journal of Electronic Materials*, vol. 46, pp. 4426–4434, 2017.

[54] M. Tadić, N. Čitaković, M. Panjan, Z. Stojanovic, D. Marković and V. Spasojevi, "Synthesis, morphology, microstructure and magnetic properties of hematite submicron particles", *Journal of alloys and compounds*, vol. 509, pp. 7639–7644, 2011.

[55] M. Tadic, N. Citakovic, M. Panjan, B. Stanojevic, D. Markovic, D. Jovanovic and V. Spasojevic, "Synthesis, morphology and microstructure of pomegranate-like hematite (α-Fe2O3) superstructure with high coercivity", *Journal of Alloys and Compounds*, vol. 543, pp. 118–124, 2012.

Received 19 March 2019